

27. R. Fricke and K. Meyring, *Z. Anorg. Allg. Chem.*, 214, 269-274 (1933).
28. A. V. Mytnikov, L. N. Shmuilov, and G. V. Telyatnikov, *Tsvet. Metall.*, No. 9, 48-50 (1978).
29. N. I. Eremin, A. N. Naumchik, and V. G. Kazakov, *Processes and Equipment for Alumina Production [in Russian]*, Metallurgiya Moscow (1980).
30. B. V. Nikogosyan and A. A. Khanamirova, *Inventor's Certificate No. 908747*, *Byull. Izobret.*, No. 8, 88 (1982).
31. L. V. Miroshnik, I. L. Boyarina, Z. I. Lobko, et al., *Ogneupory*, No. 6, 8-11 (1983).

CALCULATING THERMOELASTIC STRESSES IN A HOLLOW CERAMIC
CYLINDER WITH A LINEAR THERMAL LOADING SCHEDULE

M. I. Landa, N. N. Kopytov,
and N. M. Tsirel'man

UDC 666.762.11.017:539.4.014.11

At the present time, when the advantages of heat-resistant and refractory materials based on metals and used in aircraft components and other thermally and mechanically loaded design parts are already largely exhausted, the attention of designers, technologists, and material scientists is turning to composites and ceramics.

However, such materials are brittle, have poor heat conductivity, and inadequate thermal-shock resistance, especially in the temperature range preceding their plastic deformation. This makes it necessary to produce a precise determination of the thermoelastic stresses and temperature fields in elements of actual constructions. In this article these characteristics are studied analytically and compared with experimental results for the distribution of temperature during the determination of the thermal-shock resistance of ceramic hollow cylinders.

The authors obtained a decision in the electronic computer for the corresponding non-linear edge problem of thermal conductivity. In this case, a study was made of the temperature relationships for the thermophysical properties of the materials and the degree of blackness of their surfaces; and in limiting conditions on the external surface account was taken of the heat exchange with the surroundings according to the law of free convection and radiation, when on the internal surface of the cylinder the temperature increased with time according to the linear rule.

The temperature fields obtained in the computer were used to determine the thermoelastic stresses in the hollow cylinder assuming a quasistationary state at the moment of time being considered from the start of the thermal loading.

The solution of the edge problem for thermal conductivity includes:

- 1) the equation for the spread of heat in the hollow cylinder:

$$\bar{c}_Q(\Theta) \frac{\partial \Theta}{\partial Fo} = \frac{1}{\eta} \cdot \frac{\partial}{\partial \eta} \left[\bar{\lambda}(\Theta) \eta \frac{\partial \Theta}{\partial \eta} \right], \quad (1)$$

$$1 < \eta < 1 + \Delta, Fo > 0;$$

- 2) the simplest initial condition:

$$\Theta(Fo=0, \eta)=1; \quad (2)$$

- 3) the limiting condition corresponding to the linear temperature rise with time on the internal surface of the cylinder:

$$\Theta(Fo, \eta=1)=1+\gamma Fo; \quad (3)$$

- 4) the boundary condition corresponding to the removal of heat from the external surface of the cylinder according to the radiation-convection law:

$$-\bar{\lambda}(\Theta) \frac{\partial \Theta}{\partial \eta} \Big|_{\eta=1+\Delta} = Sk[\Theta^4(1+\Delta, Fo)-1] + \chi[\Theta(1+\Delta, Fo)-1]^{1.25}. \quad (4)$$

S. Ufimsk Ordzhonikidze Aviation Institute. Translated from *Ogneupory*, No. 10, pp. 18-21, October, 1984.

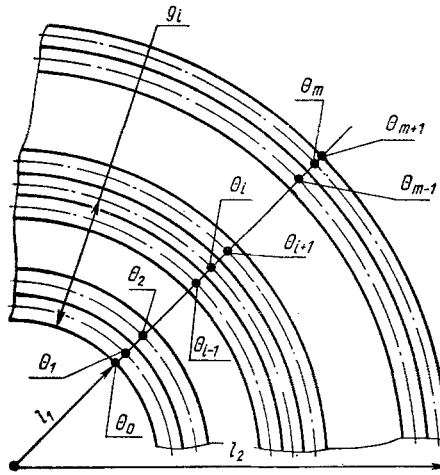


Fig. 1. Scheme for calculating the temperature field in a hollow cylinder.

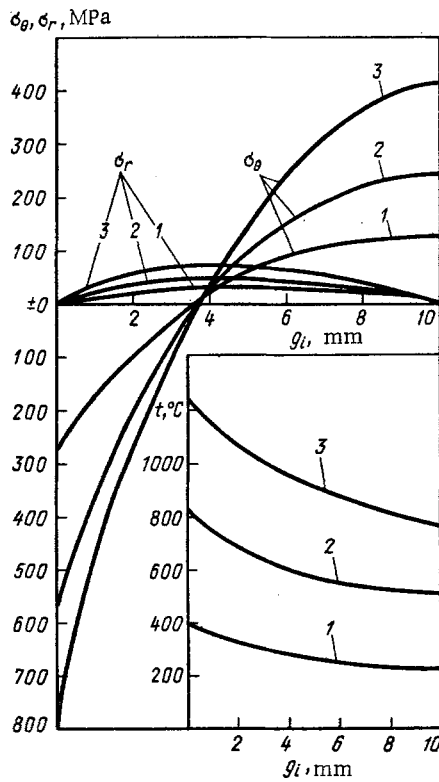


Fig. 2. Graphical interpretation of the results of calculating the nonstationary temperature field and fields of thermoelastic stresses: σ_θ and σ_r in a hollow ceramic cylinder with a thermal loading rate of $b = 5$ deg C/sec and $\epsilon = 0.3$. The thermal stress time is 80, 160, and 240 sec, respectively, for curves 1-3.

In Eqs. (1)-(4) the connotations are:

$\theta(\eta, Fo) = \frac{T(\eta, Fo)}{T_0}$ and $T(\eta, Fo)$, dimensionless and dimensional ($^{\circ}\text{K}$) current temperatures; T_0 , absolute temperature of the cylinder before the start of heating, $^{\circ}\text{K}$; $\eta = x/l_1$ and x , dimen-

TABLE 1. Thermophysical Properties of the Material

Factors	Values of factors at temp., °K							
	293	373	473	573	673	773	873	973
Rel. temp. θ	1	1,27	1,61	1,90	2,30	2,64	2,98	3,32
Thermal conductivity λ , W/(m·K)	7	5,25	4,15	3,50	3,00	2,55	2,15	1,90
Rel. thermal conductivity λ	1	0,75	0,594	0,50	0,428	0,365	0,308	0,272
Rel. volume specific heat								
$\bar{c}_Q = \frac{c_Q}{c_{Q0}} = \bar{\varphi}$	1	1,16	1,20	1,24	1,275	1,315	1,353	1,392

*Rel. degree of blackness $\bar{\epsilon}$ equals 1.

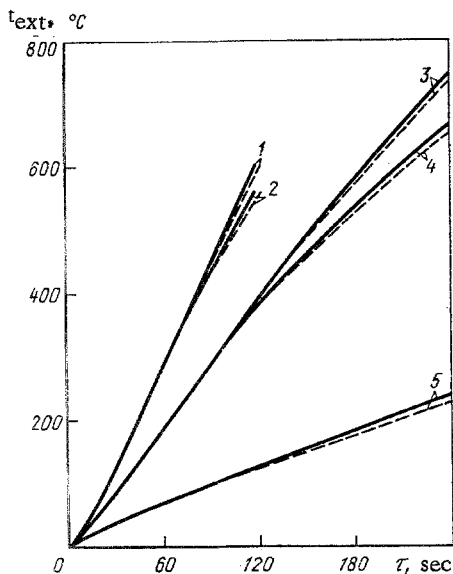


Fig. 3. Influence of ϵ on the change in time τ for temperature loading on the external surface of the hollow cylinder t_{ext}) for different rates of thermal loading: —) calculated data; - - -) experimental data; 1, 2) $b = 10^\circ\text{C}/\text{sec}$; 3, 4) $b = 5^\circ\text{C}/\text{sec}$; 5) $b = 1^\circ\text{C}/\text{sec}$; 1, 3) $\epsilon = 1$; 2, 4, 5) $\epsilon = 0.3$

sionless and dimensional, m , coordinate of the point of the body (from symmetry axis); l_1 , internal radius of the cylinder, m ; $Fo = \frac{a_0 \tau}{l_1^2}$ and τ , dimensionless (the Fourier number) and dimensional, sec , time; $\Delta = \frac{l_2 - l_1}{l_1}$ and l_2 , dimensionless thickness of the cylinder and its external radius, m (Fig. 1); $\bar{\lambda}(\theta) = \frac{\lambda(\theta)}{\lambda_0}$ and $\lambda(\theta)$, λ_0 , dimensionless and dimensional, $\text{W}/\text{m}\cdot^\circ\text{K}$, thermal conductivity of the cylinder's material, its value for T_0 ; $\bar{c}_Q(\theta) = \frac{c_Q(\theta)}{c_{Q0}}$ and $c_Q(\theta)$, c_{Q0} , dimensionless and dimensional, $\text{J}/\text{m}^3\cdot^\circ\text{K}$, volume temperature conductivity of the cylinder's material, its value for T_0 ; $\alpha_0 = \frac{\lambda_0}{c_{Q0}}$, the temperature conductivity of the cylinder's material, m^2/sec , for T_0 ; $\gamma = \frac{bl_1^2}{a_0 T_0}$ and b , dimensionless and dimensional, $^\circ\text{K}/\text{sec}$ (in relation to $T|_{\eta=1} = T_0 + br$), rate of change in temperature of the internal cylinder surface; $Sk = \frac{\epsilon c_0 l_1 T_0^3 \cdot 10^{-8}}{\lambda}$, Stark criterion, where $c_0 = 5.67 \text{ W}/\text{m}^2\cdot^\circ\text{K}^4$ is the coefficient of radiation of an absolute blackbody; $\chi = \frac{0.50 \lambda_0 l_1}{2 \lambda_0 l_2} \left[\frac{1}{T_0} \cdot \frac{9.81 (2l_2)^3}{v_n^2} Pr_0 \right]^{0.25}$, dimensionless intensity of the heat

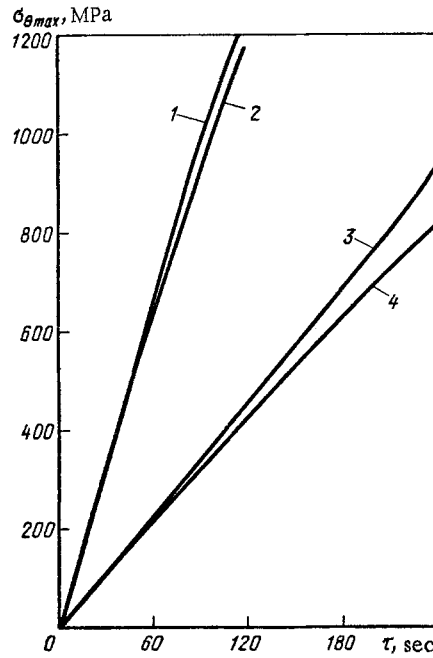


Fig. 4. Influence of ϵ on the change with time τ in the maximum thermoelastic stresses $\sigma_{\theta\max}$ in the hollow cylinder for different rates of thermal loading: 1) $b = 10^\circ\text{C}/\text{sec}$, $\epsilon = 1$; 2) $b = 10^\circ\text{C}/\text{sec}$, $\epsilon = 0.3$; 3) $b = 5^\circ\text{C}/\text{sec}$, $\epsilon = 1$; 4) $b = 5^\circ\text{C}/\text{sec}$, $\epsilon = 0.3$.

exchange with free convection of air at the external surface of the cylinder, where λ_B , ν_B , Pr_B are the thermal conductivity, $\text{W}/(\text{m}\cdot^\circ\text{K})$, and the kinematic viscosity, m^2/sec , of the air, the Prandtl criterion for air.

We note that the dimensionless intensity of heat exchange with free convection of air at the external surface of the cylinder χ was expressed on the basis of the ratio [1]:

$$\text{Nu} = \frac{\alpha_B 2l_2}{\lambda_B} = 0.50(\text{Gr Pr}_B)^{0.25} = 0.50 \left\{ \frac{1}{T_0} \cdot \frac{9.81(2l_2)^3}{\nu_B^2} [T(l_2, \tau) - T_0] \text{Pr}_B \right\}^{0.25},$$

where Nu and α_B are the Nusselt number and the coefficient of convective heat exchange present in it, $\text{W}/\text{m}^2\cdot^\circ\text{K}$; Gr is the Grashof number.

The analytical solution to the edge problem (1)-(4) in the general case in view of the nonlinearity of Eq. (1), due to the relationship between the thermophysical properties (λ , $c\rho$, α) of the cylinder's material and temperature, and the nonlinearity in the limiting conditions (4) at present is not possible.

Therefore, the solution to problem (1)-(4) is effected on the electronic computer with preliminary discretization of the spatial η and time Fo variables and the use of the implicit iterational scheme of Krenko-Nicholson [2].

As an example of actual calculations on the electronic computer ES-1022 for the problem being examined, we determined the nonstationary temperature field in a hollow ceramic cylinder made by sintering at 1200°C a thermoplasticized polyfraction powder composition based on alumina (95%) with an addition of zirconium dioxide (5%), stabilized with calcium oxide.

The cylinder dimensions were: $D_{\text{ext}} = 50 \text{ mm}$, $d_{\text{int}} = 30 \text{ mm}$, $H = 50 \text{ mm}$, i.e. $l_2 = 25 \times 10^{-3} \text{ m}$; $l_1 = 15 \times 10^{-3} \text{ m}$; $\Delta = \frac{l_2 - l_1}{l_1} = \frac{1}{3}$.

The internal surface of the specimens was heated at constant rate. The initial temperature of the hollow cylinder was $T_0 = 293^\circ\text{K}$.

The thermophysical properties of the material are shown in Table 1. The original thermal conductivity of the material was $\lambda = 8.12 \text{ W}/(\text{m}\cdot^\circ\text{K})$; $c\rho_0 = 775 \text{ J}/\text{m}^3\cdot^\circ\text{K}$.

In calculating values on the electronic computer we assumed $m = 20$, i.e., dimensionless step in space $h = \frac{\Delta}{m} = \frac{2}{3 \cdot 20}$. The step for the dimensionless time was assumed to be equal to $\tau = 10^{-3}$ ($\Delta\tau = 0.06$ sec).

In addition to studying the nonstationary temperature field, we created a subprogram of determinations for each time layer of the field of thermoelastic tensions. In this case the magnitude of the thermal stresses according to [3] was determined from the equations

$$\sigma_r = \frac{\alpha E}{\eta^2(1-\nu)} \left[\frac{\eta^2-1}{(1+\Delta)^2-1} \int_1^{\eta} t\eta d\eta - \int_1^{\eta} t\eta d\eta \right], \quad \sigma_\theta = \frac{\alpha E}{\eta^2(1-\nu)} \left[\frac{\eta^2+1}{(1+\Delta)^2-1} \int_1^{\eta} t\eta d\eta + \int_1^{\eta} t\eta d\eta - t\eta^2 \right],$$

where σ_r and σ_θ are the thermal stresses of the cylinder in the radial and tangential directions, respectively; α is the coefficient of linear thermal expansion; $\alpha = 10^{-5} \text{ K}^{-1}$; ν is the Poisson ratio, $\nu = 0.29$; and E is the elasticity modulus, $E = 1.75 \times 10^5$ MPa.

The results of the calculations for the nonstationary temperature field and the fields of thermal stresses σ_r and σ_θ in the ceramic hollow cylinder are interpreted graphically in Fig. 2. With an increase in the time of thermal loading there is a significant increase in the temperature gradient between the internal and external surfaces of the hollow cylinder and, as a result, there are increases in the thermal stresses. The sharpest increase in the hollow cylinder is shown for the tangential thermal stresses, which alter across the thickness of the wall of the specimen from compressive, in the layers adjacent to its internal surface, to tensile stresses, reaching the maximum values in its external layers.

Figure 3 shows the results of electronic-computer calculations and data of the experiment showing how there is a change with time in the temperature of the external surface of the cylinder for different thermal-loading schedules. The validity of the computerized nonstationary temperature field in the cylinder was judged by comparing the calculated and measured temperatures, naturally, only of the external surface of the specimen.

To identify the degree of influence on the nonstationary temperature field and thermoelastic stresses in the hollow cylinder of the heat-exchange conditions on its external surface we carried out computer calculations for the above characteristics of the ceramic under investigation by varying the degree of blackness of the external surface ($\epsilon = 0.3$; $\epsilon = 1$) with unaltered $\lambda = \lambda(\theta)$, $c\varphi = \varphi(\theta)$ and the same conditions of thermal loading.

The experiment was carried out on a single specimen.

After testing the original specimen with $\epsilon = 0.3$, it was cooled to room temperature without removing it from the thermal load equipment and coated with lamp black, ensuring a blackness degree on the external surface of $\epsilon = 1$. Then we again heated the specimen, fixing the change in the temperature of its external surface.

As we see from Figs. 3 and 4 the influence of the degree of blackness on the change in temperature of the external surface at 350-400°C becomes noticeable; with increase in temperature its influence rises, and moreover to a greater extent with a reduction in the rate of thermal loading. The maximum thermoelastic tensile stresses, which are the most dangerous for ceramic cylinders, with a change in ϵ from 0.3 to 1.0, increase with increase in the thermal loading time, and more intensely when $\epsilon = 1$. Thus, after 240 sec of thermal loading on the cylinder at a rate of 5°C/sec the difference in $\sigma_{\theta\text{max}}$ when $\epsilon = 0.3$ and $\epsilon = 1$ equals more than 16%.

From the above it follows that the most dangerous are the tangential stresses, which, during the transition from layers adjacent to the internal surface of the hollow cylinder to the external layers, are changed from compressive to tensile, and in the case being examined reach 400 MPa. At the same time, on the boundary of the changeover of the tangential compressive stresses to tensile a certain danger may come from the radial stresses, although their magnitude is lower than the permitted compressive strength limit of most densely sintered ceramic materials.

In the theory and practice of computing thermoelastic stresses and temperature fields in elements of actual design parts, it is necessary to bear in mind the degree of blackness

of the material since a change in it from 0.3 to 1.0, other conditions being constant, leads to an increase in $\sigma_{\text{@}}$ by a factor of three: from 420 to 1200 MPa.

LITERATURE CITED

1. S. S. Kutateladze, Principles of the Theory of Heat Exchange [in Russian], Atomizdat (1979).
2. R. D. Richtmyer and K. W. Morton, Difference Methods for Initial-Value Problems, Wiley (1967).
3. S. P. Timoshenko and D. Lessel's, Applied Theory of Elasticity [in Russian], Gostekhizdat (1930).

INVESTIGATING THE FLOWABILITY OF QUARTZITE BODIES

I. F. Usatkov and A. N. Zahkarova

UDC 666.762.2.018

The production technology for refractories, including the body preparation using the wet method, specifies that the quartzite powders and bodies be poured into hoppers; the flowability of these materials determines the reliability and continuity of the flow process.

The flowability or fluidity of the bodies was studied with the UV-70/200 equipment designed for testing articles weighing up to 70 kg on the action of vibration overloading from 0.4 to 8 g in a mechanical oscillation frequency range of from 12 to 200 Hz and an amplitude of 0.05-1 mm.

The equipment consists of a control panel and vibration rig. The vertical oscillations of the spring-mounted (vibrating) part of the vibrator are produced by the vibrator mechanism located directly under the table. The source of the oscillations consists of two imbalanced loads located on two shafts of the vibrator symmetrical to the axis, passing through the center of the table. The imbalances are rotated on the shafts in opposing directions.

The horizontal, constituent, centrifugal forces are mutually neutralizing, and the vertical constituents, in total, create a vertically directed uniformly acting force, causing oscillations of the spring-mounted part of the vibrator. The magnitude of the vertical constituent, centrifugal forces changes according to the harmonics law. Its amplitude depends on the statistical moment of the mass of the imbalances relative to the axis of the shafts and an angular velocity of the rotation.

The magnitude of the amplitude of oscillations depends on the ratio of the statistical mass of imbalance to the mass of the spring-mounted part with the load and on the frequency of the vibrations. The amplitude is determined from the equation

$$a = \frac{250P}{f^2}, \text{ hence } P = \frac{af^2}{250},$$

where a is the amplitude of the oscillations, mm; P is the vibroloading in parts of the force of gravity g ; f is the vibration frequency, Hz; 250 is the instrument coefficient of the equipment.

Using the UV-70/200 equipment we varied the vibroloading in relation to the frequency of the vibrations and the mass of the articles being tested (load).

To study the flowability of the bodies we prepared two metal hoppers: with square and rounded sections. The hoppers with the square sections were prototypes of actual hoppers used at the Pervouralsk factory, but reduced in size by a factor of 10. The hopper with the round section in its dimensions was equivalent to the square. The angle of slope of the walls of the hopper was $63^{\circ}28'$. The hoppers were equipped with removable gate valves. After carrying out a series of experiments on the metal hoppers they were lined with sheets of polystyrene. The hoppers were placed on the UV-70/200 equipment, and for each experiment we placed 20 kg of body in the hopper; without vibration this body did not flow from the hopper.